N90-28232

July 16, 1987 Revisited: Lessons for Modelers

HOWARD P. HANSON
Atmospheric and Climate Dynamics Program
Cooperative Institute for Research in Environmental Sciences
University of Colorado at Boulder 80309-0216

1. Introduction

At last summer's FSET Workshop in Vail, I presented preliminary results from 16 July 1987, the day that the NCAR Electra was allowed in the restricted air space around San Nicolas Island (NSI). We flew a cross pattern, with one leg approximately NW-SE between NSI and the R/V *Pt. Sur*, about 50 km "upstream" (although the surface winds were weak and variable), and the other leg at approximately right angles (Fig. 1). There was a LANDSAT image coincident with this mission as well. This paper discusses one interesting aspect of the "cross-stream" flight legs, i.e., the legs between points "D" and "E" in Fig. 1.

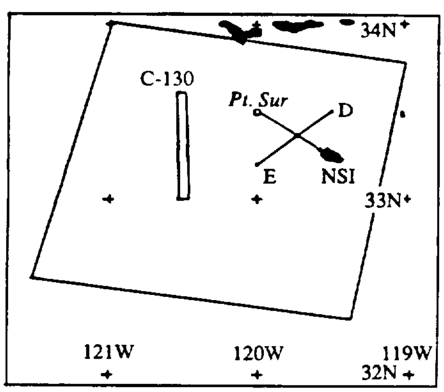

Fig. 1 FIRE operations, 16 July 1987. The NCAR Electra flew the cross pattern; the inset trapezoid is the LANDSAT scene.

The LANDSAT images (not reproduced here) show a distinct difference in cloud reflectance between the two halves of the flight leg from D (which is at the less reflective end) to E. Figure 2, which shows IR lidar observations of the cloud-top height and the reflectance calculated from the Electra's pyranometers, confirms this. Note also that that the temperature of the upwelling IR radiation is actually higher where the cloud top is higher, suggesting that the cloud is thinner there (and hence radiation from the sea surface is being transmitted). This corresponds to the less reflective part of the cloud.

What I will discuss here is the apparent reason for the variability of cloud thickness alond this flight track. The evidence points to *variability in the water vapor content above the inversion* as the controlling factor. This compounds the difficulty of parameterizing these clouds in GCM's.

2. Mixing Diagram

Figure 3, which summarizes relevant Electra data taken just above and within the cloud-topped boundary layer, is sufficiently rich in information that the remainder of this abstract will discuss it in some detail. This is a mixing diagram, plotted using total water mixing ratio and liquid water potential temperature, constructed using 1-second averages of Electra data from various altitudes. Because the two variables used are conservative to water phase changes, mixing occurs along straight lines unless there are

PRECEDING PAGE BLANK NOT FILMED

significant diabatic effects (due to, e.g., radiative transfer or precipitation).

The ellipses summarize data from the individual runs below cloud top, with the center of each ellipse positioned at the average values for each run and the axes determined using ±2 standard deviations. Each run has been broken into two segments, corresponding to the less (segments 1) and more (segments 2) reflective parts of the cloud. The surface data ellipse (labeled "S") was determined using the radiometric sea-surface temperature (SST) and the associated saturation vapor mixing ratio (the SST varied little between D & E, and this is not segmented). Proceeding generally down and to the right, the other data ellipses are from flight legs at 60m, 475m (the base of the cloud layer), and 675m (in the middle of the cloud layer. The asterisks (circles) are 1-second data points from the cloud top run corresponding to segment 1 (2), during which we "porpoised"

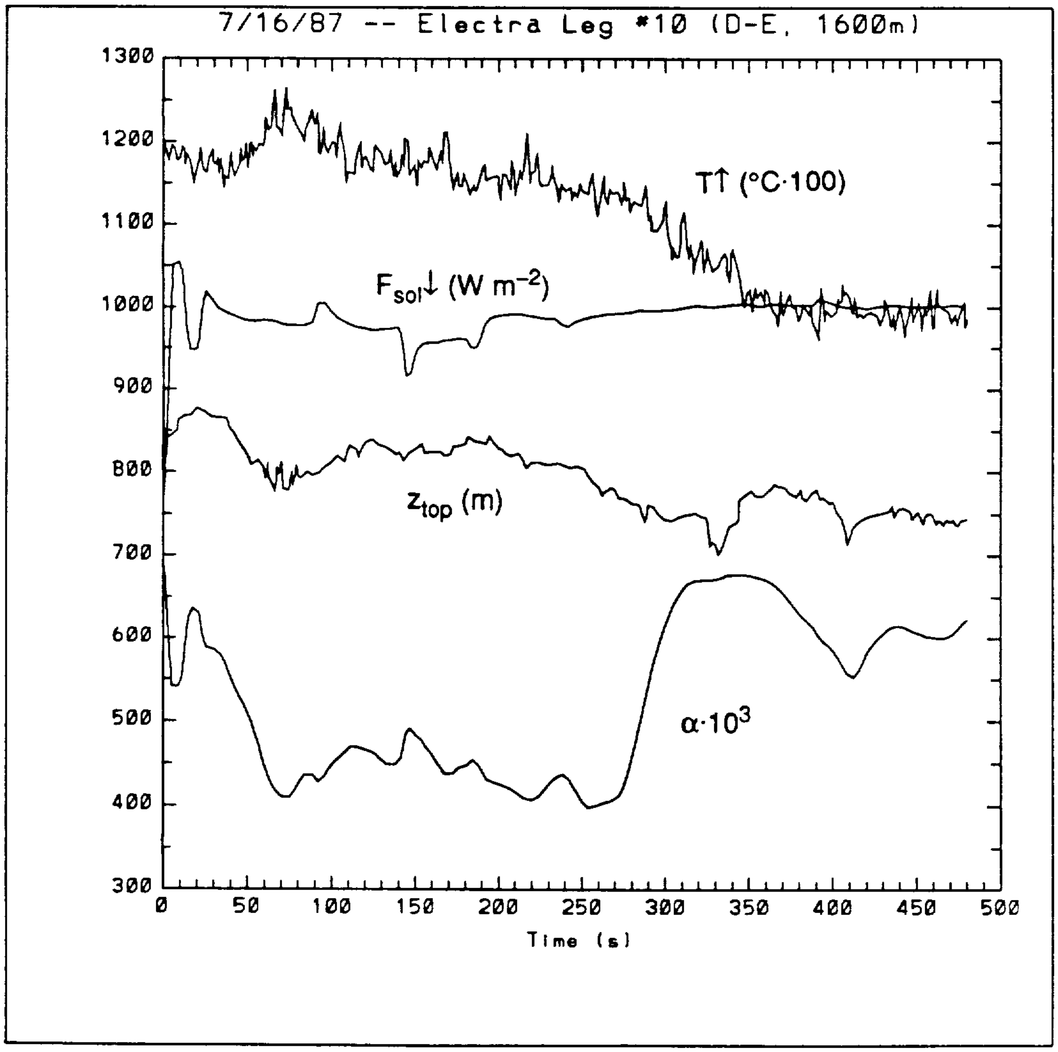

Fig. 2 Downward solar radiation $F_{sol}\downarrow$, cloud reflectance α, upwelling IR radiation (in terms of its temperature $T\uparrow$)) and cloud-top height z_{top}, along the flight leg from D to E in Fig. 1.

in and out of the cloud top (as can be seen in the altitude data [solid] in Fig. 4).

Although the cloud was evolving during the mission, these manuevers took only about an hour to complete, so that the data are nearly "synoptic" in terms of the time scale of the cloud. Because of this, several conclusions can be drawn from Fig. 3. First, it can be argued that the sub-cloud and cloud layers were decoupled. Consider the mixing line between the surface air and that at cloud base. There is clearly a discontinuity from this line to the (two separate) in-cloud parcels. Also, the displacement of the 60-m air parcels from the subcloud mixing line can be accounted for by a radiative cooling rate of ~ -0.5°/day, a very reasonable value.

If the layers were decoupled at the time of the measurements, then the surface moisture supply for the cloud was cut off, and entrainment of warmer air

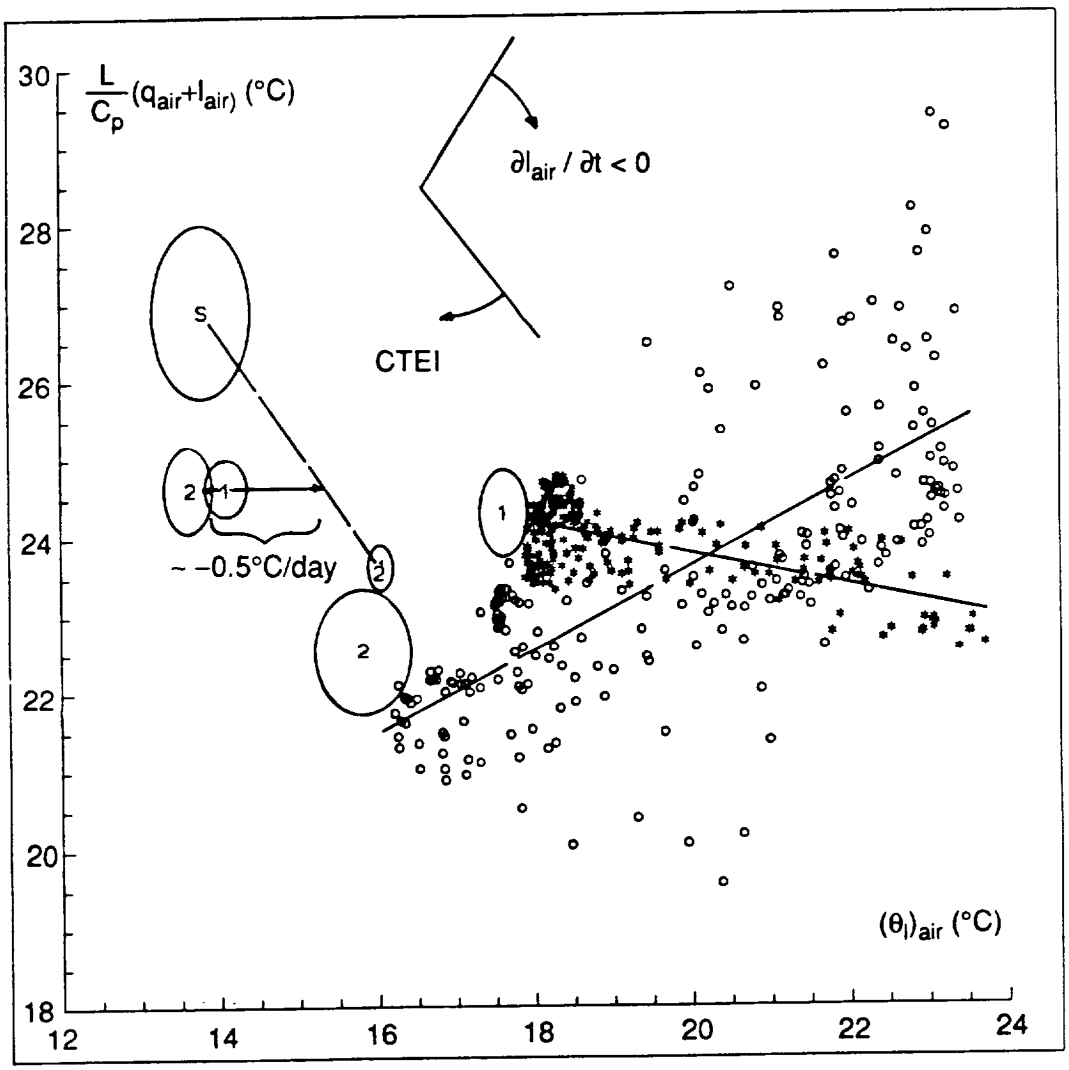

Fig. 3 Mixing diagram summarizing data between points D and E.

from above combined with solar heating (which probably lead to the decoupling in the first place) would tend to decrease the liquid water content of the cloud.

Note, however, the difference in the moisture content of the air above the inversion between segments 1 & 2. The dashed lines through the asterisks and circles in Fig. 3 are regression lines of these data points, and therefore are the best estimate of the mixing line for entrainment in the two segments. The difference in the slope of these two mixing lines is highly significant.

At the top of Fig. 3, there are indicated two critical mixing lines. Cloud-top entrainment instability occurs for mixing lines having slopes less than (i.e., more negative than, or clockwise from) the line marked "CTEI". Clearly, that is not happening in the data. The other line is a mixing line for which entrainment would produce no change in cloud liquid water; mixing lines with smaller slopes

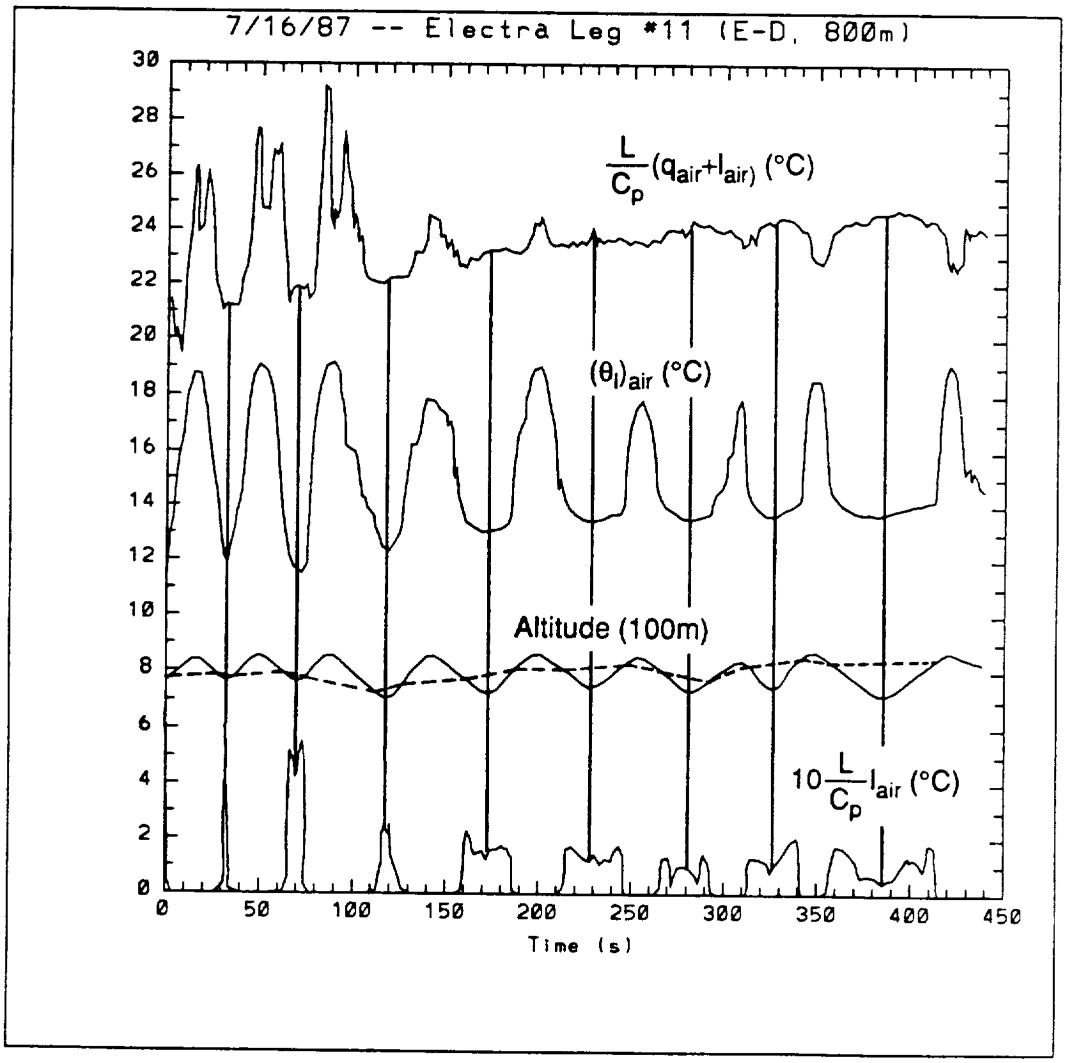

Fig. 4 Aircraft altitude, liquid (l_{air}) and total water (q_{air}+l_{air}) mixing ratios, and liquid potential temperature θ_l from cloud-top leg. Dashed line estimates cloud top from the liquid water data.

(in the same sense as previously) tend to decrease the cloud liquid water, and the rate of liquid water decrease is proportional to the difference in slope.

The difference in slope of the two regression lines is, in this context, highly significant. Although both imply mixing by entrainment that decreases the cloud liquid water, the segment 2 mixing (the circles) produces only about half the decrease of the segment 1 mixing. In fact, for segment 2, the *above-inversion air is acting as a moisture source for the cloud layer*.

3. Conclusion

The main point here is the importance of specifying correctly the upper boundary condition in cloud models. This example shows that relatively small variations in the humidity of the air above the marine inversion can be lead to variations of cloud reflectance by as much as 50% (about 0.4 to 0.6, here). The relatively small scales of this phenomenon in this data set (O[25 km]) are less important that the magnitude of the reflectance variability. Particularly in GCM's, calculating the humidity in the lower layers of the model is crucial for successful parameterization of marine stratocumulus clouds.

Acknowledgments: This research was supported by the Office of Naval Research and the National Aeronautics and Space Administration.